Journal of Hazardous Materials 480 (2024) 136126

Contents lists available at ScienceDirect

Journal of Hazardous Materials

journal homepage: www.elsevier.com/locate/jhazmat

Exploring microplastic distribution in Western North American snow

Aleksandra Karapetrova [a,*], Win Cowger [a,b], Alex Michell [c], Audrey Braun [a], Edward Bair [d], Andrew Gray [a], Jay Gan [a]

[a] Department of Environmental Science, University of California, Riverside, CA 92521, USA
[b] Moore Institute for Plastic Pollution Research, Long Beach, CA 90803, USA
[c] Airborne Snow Observatories, Inc., Mammoth Lakes, CA 93546, USA
[d] Leidos, Inc., Reston, VA 20190, USA

HIGHLIGHTS

- Atmospheric deposition of microplastics was found in remotely located snow.
- Microplastics were detected in 11 sites across western coastal North America.
- Concentrations of microplastics in snow ranged from 5.1 p/L-914 p/L of meltwater.
- Detection of microplastics < 100 μm was done using μFTIR mapping and OpenSpecy.

GRAPHICAL ABSTRACT

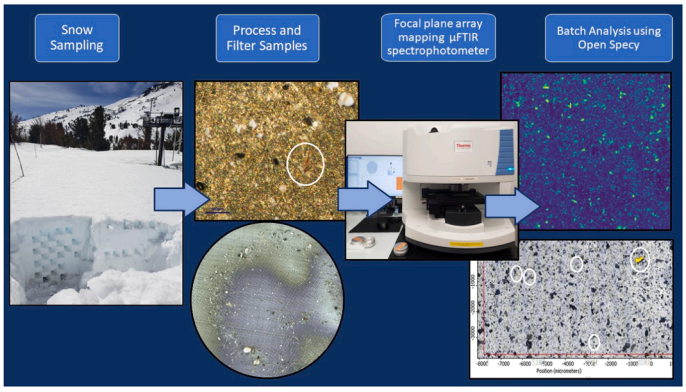

ARTICLE INFO

Keywords:
Microplastic
Snow
Atmosphere
Long-range Transport
Environmental microplastics

ABSTRACT

Microplastic (MP) transport in the atmosphere, one of the least studied environmental compartments because of the relatively small size of air-borne MPs and the challenges in identifying them, may be inferred from their occurrence in snowfall. In this study, 11 sites across western coastal North America were sampled and analyzed for MP presence in fresh snowfall, months-old summer surface snow, and stratified deposits in snow pits. MPs were detected and characterized using a method integrating linear array μ-Fourier Transform Spectroscopy (μFTIR) and batch spectral analysis with open-source platform Open Specy. Recovery rate analysis from sample filtration to data analysis was conducted, and analysis of field or laboratory blanks suggested negligible contamination (≤ 1 polyamide fragment per blank). Concentrations of MPs in the fresh snowfall of remote sites and those proximal to sources were 5.1–150.8 p/L and 104.5–325 p/L of snowmelt water, respectively. Summer surface snow that was several months old had MP concentrations ranging from 57.5–539 p/L of meltwater, and snow sampled at different depths within a snowpack had concentrations ranging from 35–914 p/L. Our results demonstrate a streamlined method that may be used for measuring MPs in remote or pristine environments, contributing to a better understanding of long-range MP transport.

* Corresponding author.
E-mail address: akara032@ucr.edu (A. Karapetrova).

https://doi.org/10.1016/j.jhazmat.2024.136126
Received 2 August 2024; Received in revised form 1 October 2024; Accepted 8 October 2024
Available online 10 October 2024

1. Introduction

The global production of plastic products and the mismanagement of waste over the course of many decades have led to the omnipresence of microplastic particles (MPs) in ecosystems, including those that are remote from human activity. [1–3] Of all the plastic that is no longer in use, only 9 % has been recycled, leaving the rest to be either discarded or incinerated. It is estimated that by 2050, 12 billion metric tons of plastic will have been discarded. [4,5] Furthermore, the current estimated global production of plastic waste per year is over 350 million tons and is projected to be over 1 billion tons by 2060. [6] With the increase in production of plastics, the generation of plastic waste and MPs will follow. MPs have been found in all environmental compartments; however, at present, among the different environmental compartments, MP presence in the atmosphere is relatively poorly understood. [7,8] Atmospheric MPs may pose a unique risk because of exposure via inhalation or ingestion, the amplification of their transport due to meteorological events, and aging of MPs while in the atmosphere leading to changes in their surface characteristics and properties. [9,10].

Evaluation of MP occurrence and accumulation in remote regions by sampling snow can contribute to a better understanding of the role that atmospheric transport plays in the global cycle of MPs. [11] Environments with snowfall offer a unique venue for understanding MP occurrence in the atmosphere because of the frequent atmospheric condensation and scavenging phenomena. [12,13] When atmospheric MPs undergo environmental aging processes, the surface of the particles become more hydrophilic, thus becoming more favorable cloud condensation nuclei and ice nucleus particles. [14–16] Additionally, below-cloud scavenging is a process that could be an especially effective mechanism capturing MPs from the atmosphere because of the large surface area of snow condensation. [17,18] During the in-cloud scavenging of particles, MPs may serve as cloud condensation nuclei. [19] Snow particle terminal velocity decreases with the increase in size, allowing for scavenging to be up to 50 times more efficient than rain based on the snow water equivalent of a snow particle to a raindrop. [10] The deposition of MPs is a dynamic process, as resuspension to the atmosphere due to surface-level turbulent processes can occur. [20] It is estimated that the current average total atmospheric burden of MPs over the land regions of the western United States is 10,000 kg; however, little is known about the environmental fate of such atmospheric MPs. [21] The presence of MPs in areas with no proximal anthropogenic activity reveals that atmospheric processes are responsible for long-range transport of MPs which is further supported by extensive modelling [22, 23].

In the western United States, the snowpack acts as an important reservoir for fresh water, and its significance will no doubt increase further in the coming years due to climate-induced changes in precipitation patterns. [24] For example, in California where 39 million people live, up to a third of the state's water supply comes from the snowpacks in the Sierra Nevada. [25] Therefore, understanding anthropogenic contamination of snowpacks by emerging contaminants such as MPs is also important to ensure the integrity and safety of future water resources. Environmental contaminants like MPs can travel in snowpack run-off and traverse over long distances through watersheds. [26] Atmospheric deposition of MPs in the snowpack may have multiple directions of transport; for example, they may be resuspended in the atmosphere from the snowpack, accumulate in the soil, move offsite through runoff, and even enter organisms through inhalation or ingestion in the alpine environment [27].

The limited research into MPs in the atmosphere may be attributed to the fact that it is highly challenging to measure atmospheric MPs because of their small sizes ($<$ 300 μm). [9] Snow is likely a more preferable matrix for detecting atmospheric MPs because of the relatively low amount of organic matter co-existing in the sample. This potentially allows for lower chances of false positive MP detection from organic matter, while less particle crowding on filters may also facilitate collection of spectroscopy data. [28] Sampling above the tree line, where plants are typically covered by the snowpack, further reduces chances of false positive MP detection. [29] In addition, in the snowpack, snowfall events are stratified in visible layers, which provides opportunities to understand accumulation trends of atmospheric MPs on a timescale [30].

A few studies of limited scope have reported MP in snow with concentrations varying several orders of magnitude. This can not only be attributed to site-specific environmental processes, but also differences in data collection methods. [31] Sampling in snow-dominated environments can provide evidence for long-range transport of atmospheric MPs. [32–35] For example, similar MP concentrations have been reported in the snow of Antarctica and Mount Everest (29 and 30 p/L, respectively). [1,36] Even lower concentrations were found in the Italian Carnic Alps (0.11 p/L). [37] Remote regions that had substantially higher concentrations included Arctic snow in Svalbard (1.76×10^3 p/L) and the Tibetan Plateau in China (650–920 p/L). [2,38] In addition to snow, MPs of mostly hydrophilic polymers have been detected in cloud water from the free troposphere and atmospheric boundary layer (6.7–13.9 p/L) on Mt. Fuji, suggesting that cloud condensation nuclei formed around the particles. [15] Another study on cloud MPs, in contrast, reported a higher average of MPs (463 p/L) on Mt. Tai, and the higher occurrence may be due to the presence of more proximal anthropogenic sources than that around Mt. Fuji. [39] Among these studies, the size detection limits, snow densities, and sampling and MP detection methods were all different. However, among published studies, one common influence on MP abundance is the relative proximity to anthropogenic activity.

The use of μFTIR mapping can eliminate the difficulty of detecting MPs among atmospheric particles. This approach was first introduced over five years ago, but to date few studies have applied this technique to environmental samples. [40–42] Focal plane array mapping has the potential for high-throughput detection of environmental MPs. This method may be especially useful for atmospheric deposition samples where the majority of MPs are under 100 μm in size and would be nearly impossible to identify using visible light and human particle-picking techniques. [43].

In this study, an improved method integrating an automated detection technique with focal plane array mapping on a μFTIR and spectra batch analysis Open Specy for the identification and measurement of atmospheric MPs in snow samples was introduced. [44] The field observations on the abundance and patterns of MP occurrence in California, Oregon, and Alaska snowpacks were compared to the other remote regions around the world. The presence of MPs in areas remote from human activities contributes to the understanding of global long-range transport of MPs. [43,45] In addition, it is anticipated that the detection method and proposed workflow may be valuable in future research for rapid and reliable determination of small-sized MPs in various environmental samples.

2. Materials and methods

2.1. Study sites and sampling

Between August 2021 and April 2022, sites in Mount Hood National Forest in Oregon, USA, Inyo National Forest in California, USA, and the Seward Peninsula of Alaska, USA, were visited on foot or using skis for sample collection (Fig. 1). Permits and letters of nominal use were received before sampling from the respective National Parks and Forests Special Permit offices. Specific sampling locations were selected based on the alpine elevation (above tree line), even snow deposition, distance from trees (greater than 70 m), flatness of ground, and safety in accessibility. Maps of the sampling sites are shown in Fig. 1, with more details given in Table 1.

The overall workflow for sample collection, sample processing and MP identification is summarized in Fig. 2. Two methods were used to

collect snow samples. A snow grab technique was used for perennial snow on glaciers and fresh snow, while a manual snow density measurement technique was used for snow in the winter season (Table 1). Snow grabs were performed by measuring 35 cm × 35 cm square and shoveling surface snow at 2–3 cm depth into a sampling bottle. For snow sampling using the manual snow density measurement technique, a snow pit was dug, and samples were taken at 10-cm increments to maximum snowpack height of 110 cm. The volume and density of snow were recorded for both snow pit samples and freshly deposited snow.

Manual snow density measurements were taken using a Pro Snow Kit I (Snowmetrics, Fort Collins, CO), and all snow samples were collected into 2 L unpainted stainless-steel bottles (EcoTanka, Waikato, New Zealand). All bottles were washed with sea wool and a mild detergent and then triple rinsed with ultrapure water that had been filtered through a Whatman Grade GF/A 47 mm glass fiber filter (Cytiva, Amersham, United Kingdom). Grab samples were collected with an aluminum avalanche shovel with no paint coating (Mammut Sports Group, Williston, VT). Biodegradable waxes were used on skis and skins to prevent cross-contamination (Mountain Flow Ecowax, Denver, CO). Sample collectors wore lab coats (Fisherbrand, Waltham, MA) that were 100 % cotton and dyed purple (Rit liquid dye, Indianapolis, IN) to identify possible contamination in samples. All shirts worn were made of

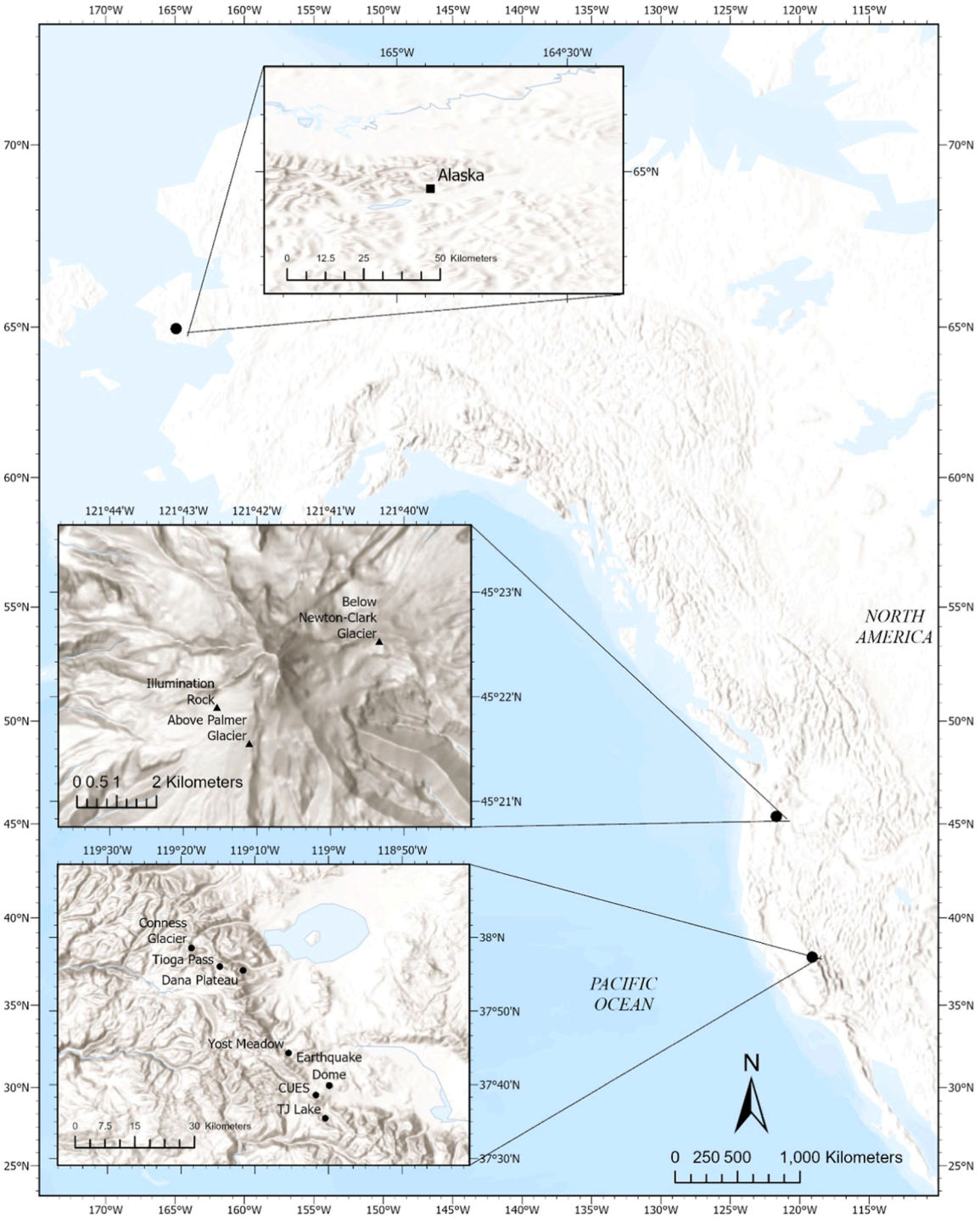

Fig. 1. Locations of sampling sites on the West Coast of North America. Maps were created using ArcGIS Pro (version 3.1.3).

Table 1
Description and location of sampling sites in this study.

Site name	Coordinates (N°, W°)	Elevation (m)	Type of snow sample	Distance from anthropogenic source (km)
Earthquake Dome	37.66474, −118.99857	2851 m	Fresh[a]	3 km
Yost Meadow	37.73864, −119.08982	2819 m	Fresh	5 km
Dana Plateau	37.92545, −119.19354	2896 m	Fresh	7 km
TJ Lake	37.590622, −119.007130	2818 m	Fresh	4 km
Tioga Pass	37.934114, −119.245959	2914 m	Fresh	11 km
Alaska	64.950, −164.902	183 m	Fresh	60 km
CUES	37.64328, −119.02911	2938 m	Fresh/Pit[c]	1 km
Above Palmer Glacier	45.359281, −121.701740	2613 m	Summer seasonal[b]	8 km
Below Newton-Clark Glacier	45.375586, −121.672293	2469 m	Summer seasonal	11 km
Conness	37.97633, −119.30960	3292 m	Summer seasonal	16 km
Illumination Rock	45.365073, −121.709024	2698 m	Summer seasonal	8 km

[a] Fresh snow samples were collected within 24 h of deposition. [b] Seasonal summer snow samples were collected as a surface snow grab on seasonal snow that had not yet melted from the previous winter and spring season. [c] Pit snow samples were samples taken along the depth of a snow pit using the manual snow density measurement technique.

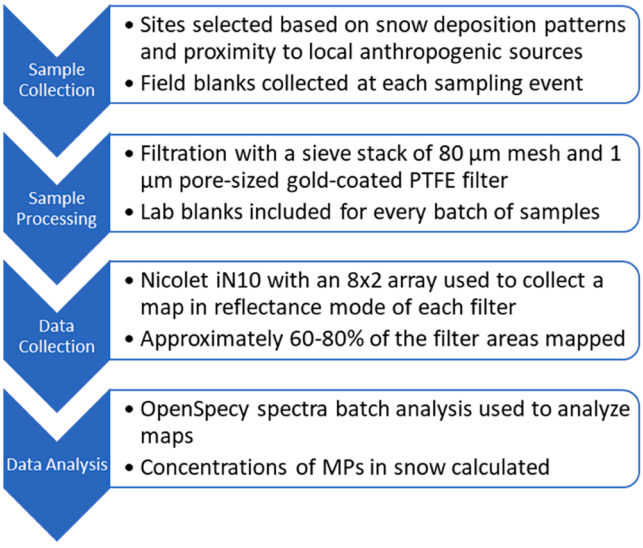

Fig. 2. General workflow of sample collection and measurement of MPs in snow samples.

merino wool (Smart Wool, Steamboat Springs, CO and Ridge Merino, Mammoth Lakes, CA). Individuals collecting samples stood downwind of the snow pit to minimize possible contamination. The color of all outerwear was recorded in notebooks in case of potential plastic contamination. Before sample filtration, all samples were transferred to wide-mouth amber glass bottles (Berlin Packaging, Chicago, IL) that were washed with the same procedure as the sampling bottles. Glass bottles were corked with natural laboratory-grade cork (WidgetCo, Houston, TX) to prevent possible plastic contamination from plastic lids. At all sites, meteorological data were measured using a Kestrel 5500 weather meter (Nielsen-Kellerman, Boothwyn, PA). Samples collected at the Cold Regions Research and Engineering Laboratory and the University of California Santa Barbara Energy Site (CUES) (Fig. 1C) had accompanying meteorological and snowpack data recorded by instruments at the site [46].

Samples were defined by the type of snow collected at the site, location, and proximity to concentrated anthropogenic activities (Table 1). Point sources were defined as a community with a population greater than 5000 people. Sites were not remote if there was a local point source of MPs within 3 km. Sites were considered remote if they were greater than 3 km in direct distance from an anthropogenic source. The samples collected within 3 km of a local anthropogenic source included those from the CUES site. The localized anthropogenic sources at the CUES site included the Mammoth Mountain Ski Area and the town of Mammoth Lakes. Although the snow plot did not have immediate human activity, it was located close to the ski resort, where many people were moving with polymer-based clothing; in addition, a road circumnavigates the area. A pit was dug at the snow plot before the snowpack was isothermal, and fresh snow was regularly sampled there throughout the winter season. The 110–100 cm and 60–50 cm layers (layers measured in height from the ground surface) in the pit collected on March 24, 2022, both included crusts and faceted snow, which signified periods of dry deposition. The 110–100 cm layer coincided with the driest 3-month period on record in California and at the CUES site. [47] The 60–50 cm layer included a dry period lasting from mid-November to late-December in 2021. The surrounding remote sites at which fresh snow was collected were TJ Lake, Earthquake Dome, Yost Meadow, Dana Plateau, and Tioga Pass. The TJ Lake and Earthquake Dome sites were both < 5 km from local anthropogenic sources, the same local point sources as the CUES plot.

Summer snow sites were Illumination, Above Palmer Glacier, Below Newton-Clark Glacier, and Conness. All summer snow sites were classified as remote, but there were some hiking trails and summer ski resorts within 3 km.

2.2. Sample processing

All samples were processed in a laminar flow hood (NuAire, Plymouth, PA). Before filtering snow melt samples, the hood was wiped down with rubbing alcohol and wipes (Kimtech, Neenah, WI). The surface of all glass amber bottles and sampling bottles were wiped down with wipes. A purple-dyed cotton lab coat was always worn when filtering snowmelt samples. An all-glass vacuum filtration set (Advantec MFS, Dublin, CA) was used for filtration, and the funnel was always covered with aluminum foil in between pours. Volumes of filtrate were recorded to determine snow water equivalents and compared against measurements taken in the field.

Snowmelt water samples were first filtered onto 80–120 µm stainless steel meshes with a straight weave (McMaster-Carr, Elmhurst, IL) that were punched into 25 mm diameter circles using a 1-inch puncher (Grainger, Arlington Heights, IL). This sieving step was intended to capture large particles that may clog the 0.8 µm gold-coated PTFE. The filtrate was then poured onto a 0.8 µm gold-coated PTFE filter. Vacuum pumps were operated at 50 L/min. Gold-sputtered filters were made in the laboratory using 1.0 µm polycarbonate filters (Sterlitech, Auburn, WA) by sputter coating each side for 120 s at 30 mA using a Cressington 108 Auto sputter coater (Cressington Scientific Instruments, Watford, United Kingdom). The filters were stored separately in pre-washed and triple ultrapure water rinsed tin containers before use.

2.3. Spectra collection and Open Specy software analysis

The iN10 Nicolet µ-FTIR with linear array mapping was used in reflectance mode (Thermo Fisher Scientific, Waltham, MA), and a map of a 144 mm^2 area (12 mm × 12 mm square) was collected on each mesh and gold-coated PTFE filter. All spectra were collected in reflection mode, and spectra format was saved as absorbance. Background spectra

were collected before each scan, at a custom collection time of 512 scans. The scan speed was set to fast speed and signal filter set to Black-Harris. No corrections were applied to the spectra. Spectra were collected at 25 μm steps, so approximately 300,000 spectra were collected on each filter. Fibers under 25 μm thickness were found on the 80-μm stainless steel mesh filters by visual comparison and were identified using the Omnic Picta software (Thermo Fisher Scientific).

Open Specy is an open-source infrared spectra analysis software and a library of spectra. [44] Once spectral maps were collected using the μFTIR, the high dynamic range (HDR) and DAT files of each map were converted to a ZIP file for analysis by the Open Specy R package. The batches were analyzed using RStudio 4.2.2 and the Open Specy spectral R package. [48] Signal-times-noise particle thresholds were defined by a 0.045 ratio. Continuous regions with particle spectra were merged into a single spectrum for each particle using the median of the spectral signals. The Open Specy "mediod" library was then used to correlate spectra from the maps to the library. The correlation coefficient with the Open Specy library was a minimum of 0.7 for each spectrum, and two adjacent spectra of the same polymer class were required to generate a true value for an MP particle. Although these parameters might potentially exclude small particles, they minimize the potential for false positives in the samples. Due to these parameters, the lower particle detection limit of this method was a 50 × 25 μm particle size. Generating plots and data for each map of about ~270,000–300,000 spectra took less than 10 min per map.

R studio-generated plots of particle thresholding and polymer classification were saved for each filter. Supplementary material data and R code generated from analysis was uploaded to an open source data repository. [49] To ensure proper particle thresholding, polymer classification plots with a transparent background were overlayed onto visible light mosaic images. By visual comparison, the overlay verified accuracy with Feret min, Feret max, and particle count output from the Open Specy software. Data output of particle size, correlation coefficient, particle coordinates on the map, and polymer type were saved from the "cleaned_matches" output generated from the software. "Cleaned matches" were MP particles that were true values based on the aforementioned parameters defined in the code. From this list of "cleaned matches", data particle counts, MP concentrations on filters, fresh snow, and meltwater were generated and statistical analysis was performed on this data.

In order to verify the presence of fibers in addition to a visible light mosaic image generated by the μFTIR, 80-μm meshes were photographed using a Color Nikon Camera DS-Fi3 camera (Nikon, Melville, NY) at 31.5x magnification. These high-resolution images allowed for thorough fiber identification and documentation of fiber counts on 80 μm pore-sized meshes.

2.4. Calculation of MP concentrations

The "cleaned_match" data was exported into Microsoft Excel, and the MP particle counts on each filter and the concentrations of MP particles in snow and meltwater were extrapolated using the following equations. Equation (1) was used to calculate the concentration of MP particles on each filter. In general, the particle distribution seemed to be even on the 0.8-μm filters. A square map of 12 × 12 mm was scanned for each 25 mm filter such that the edges and center of the filter were within the map area. The filtration area on most filters was about 201 mm^2 as the inner diameter of the funnel in the filtration set-up was 16 mm. Therefore, about 72 % of each sample filter was scanned with FTIR.

$$C_{MP\ \ \text{particles on filter}} = \frac{P_{\text{detected on map}}}{A_{\text{map}}} \times A_{\text{filtratration on filter}} \quad (1)$$

A denotes the area of the filter measured, P denotes the particle count of MPs detected, and C denotes the concentration of MPs extrapolated for the sample. The volumetric concentration of MPs was calculated for meltwater using the following equation:

$$C_{MP\ \ \text{particles in meltwater}} = \frac{C_{MP\ \ \text{particles on filter}}}{V_{\text{filtered snowmelt}}} \quad (2)$$

where V is the volume of snowmelt filtered onto the 80 μm mesh and 0.8 μm gold PTFE filter.

To make direct comparisons of MP concentrations in snow between snow samples, the snow water equivalent (SWE) of each snow sample was calculated and then multiplied by the concentration of MPs in meltwater that was calculated in equation (3):

$$C_{\text{MP}\ \ \text{particles in snow}} = C_{\text{MP}\ \ \text{particles in meltwater}} \times \frac{M_{\text{1L snow}}}{V_{\text{1L meltwater}}} \quad (3)$$

Here, the density of the snow collected was measured in the field using a snow density cutter of known volume and weight of the snow. The density of sampled snow varied from approximately 100 to 450 g/L, which corresponds to approximately 10–45 % SWE.

2.5. Quality assurance and quality control

All sample sites were sampled in duplicate, and a blank was collected for each sampling event at a site. The weight of samples and equipment were a limiting factor for the sample volume that could be transported back to the laboratory. Field blanks were pre-washed and pre-rinsed stainless steel sampling bottles that were placed open at the sampling pit while the sample collector mimicked the motions of sampling into the sampling bottle. Once brought to the laboratory, the field blanks were rinsed with ultrapure water 3 times, and the rinse water was filtered onto a 0.8 μm pore-sized gold-coated PTFE filter (Sterlitech, Auburn, WA) to measure field site contamination. The rate of contamination from the field was an average of 1 polyamide fragment per blank. Laboratory blanks were collected inside the fume hood where all samples were processed. Laboratory blanks were collected by mimicking the actions used in the processing of a sample, including the motions, time, and ultra-pure water rinsing. The rate of contamination from the laboratory blanks was an average of 0.3 polyamide fragment per blank. A recovery rate experiment was performed in triplicate with 250–300 μm blue polyethylene spheres and 70–90 μm red polyethylene spheres (Cospheric, Goleta, CA). The recovery rate of 250–300 μm blue MPs from filtration to data analysis was an average of 98 % and 70–90 μm red spheres an average of 76 %. These recovery rates meet or are above the standards for MPs in drinking water measurement protocols for California Statewide MP testing. Pristine polyethylene spheres are hydrophobic, behaving significantly different than environmental samples in the filtration process and can become crushed to powdered fines during the filtration process. This makes it difficult for recovery rate experiments to be representative of environmental sample recovery rates. Before measuring filters of environmental samples, a series of positive and negative controls were measured (Fig. 3). The significance of these measurements was to ensure confidence in the detection of MPs in environmental samples and set an appropriate signal to noise ratio for the environmental sample measurement. All filters used in this control experiment were gold-coated PTFE 0.8-μm filters. A series of filters with LDPE particles of sizes 40–48 μm were filtered onto a gold PTFE filter, and then the particle count, type, and size were determined to understand the accuracy of the Open Specy analysis. The filter had considerable crowding and particle touching, so the automatic particle count was an underestimation. The analysis showed that all the particles were of the same polymer class (LDPE) and consistently had correlation factors > 0.7 with the "mediod" Open Specy library. In another test, pine needles were gathered from the CUES site and cryomilled with liquid nitrogen into fine particles, mixed with ultrapure water, and then filtered onto a gold PTFE filter. The purpose of this test was to ensure that no false positive matches arose from the presence of plant material surrounding the sampling sites. Plant materials may generate false positives with polyamide spectra in plastic spectral libraries. [50] At all the sites, the most common plant material that could generate false positives in

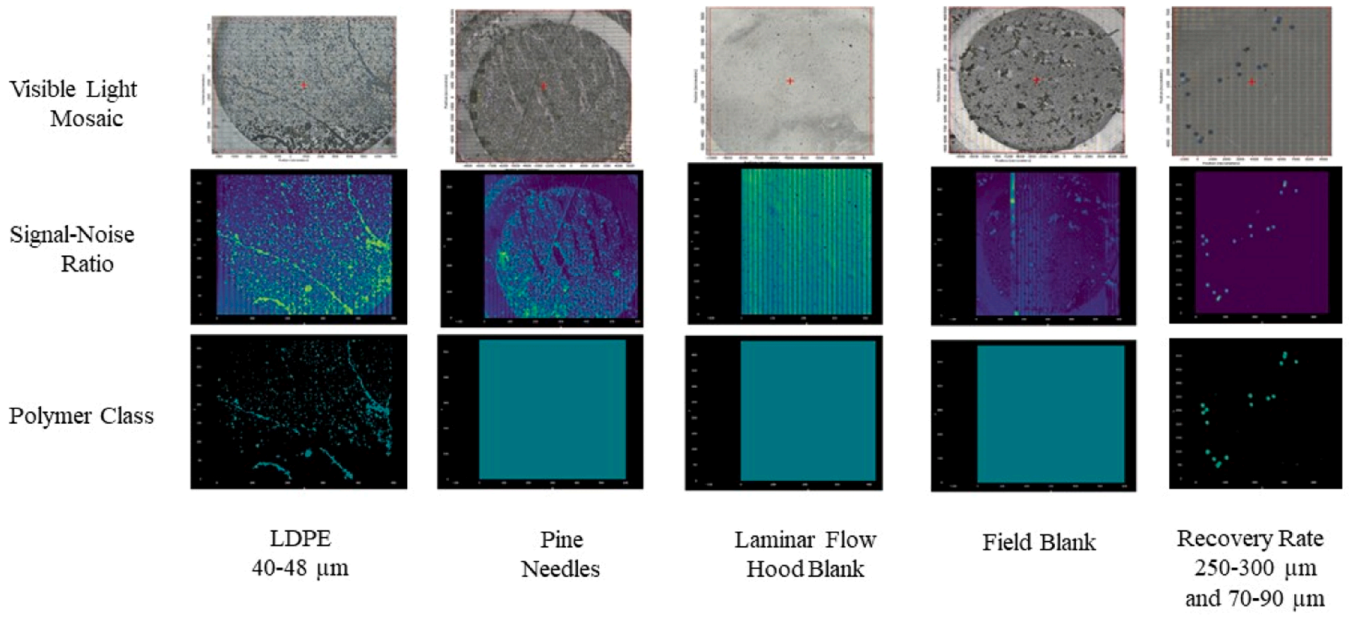

Fig. 3. Validation of LDPE particle positive control, potential false positive (pine needle material), an example of two blanks that did not have MP presence from the laminar flow hood and the field blank, and a recovery rate experiment. The visible light mosaic was generated from Omnic Picta, and the signal-noise ratio and polymer class plots were generated on RStudio using the Open Specy software package.

the measurements was pine, as it was the only plant not submerged by the snowpack at the time of sampling. Using the Open Specy library, it was shown that the cryomilled pine material did not generate false positives.

2.6. Statistical analysis

Sample sites were grouped into four classes, i.e., remote fresh snow, remote summer snow, fresh snow at CUES, and snow from a pit at CUES. Two-way ANOVA, one-way ANOVA, and Dunnet's T3 multiple comparison tests were performed using GraphPad Prism (version 10.0.0 for Windows). Statistically significant differences in size and polymer type distributions, and MP concentrations between the four types of sample sites ($p < 0.05$) were tested. Data on MP particle concentrations, polymer class counts, and MP particle area sizes were imported into Graph Pad Prism for plotting and statistical analysis.

3. Results

3.1. Concentrations of MPs in snow meltwater

Among the 24 samples analyzed, a total of 715 MPs were detected using the workflow presented in Fig. 2. Calculation of the concentrations of MPs at multiple geographic sites provides a baseline for the presence and distribution of MPs across multiple areas (Table 2). Due to instrument detection limitations, only MPs that were at least 50 µm in Feret diameter were observed and identified as plastic. MPs were observed at all sampling locations.

The concentrations of MPs found in the fresh snow of remote sites (n = 9) varied from 5.1–150.8 p/L of snowmelt water, while the MP concentrations varied from 104.5–539 p/L in snowmelt water of fresh snow collected at the CUES site (n = 6) (Fig. 4). Of the remote sites, 8 were in the Sierra Nevada range in California, and one was in the arctic tundra in Alaska. There was a significant difference (Dunnett's T3 multiple comparison test) in concentrations of MPs in freshly deposited snow between the remote sites and the CUES site ($p = 0.038$). However, there was no significant difference in meltwater concentrations of MPs between the remote fresh snow sites and remote summer snow sites or CUES pit samples.

Meltwater concentrations of MPs in remote summer seasonal snow varied from 57.7–529 p/L. Of the 5 samples, 4 were sampled from Mt. Hood in Oregon, and 1 sample was from the Sierra Nevada in California. Despite being considered remote, the Conness site, a popular path to an alpine climbing destination, had the highest concentration of MPs.

In this study, from the snow pits dug at the CUES site, the MP concentrations varied from 35–913 p/L of meltwater. The sample collected at 110–100 cm from the ground surface on 03/24/2022, which had the highest concentration of MPs in meltwater, included a crust layer of the longest dry period recorded in California history.

3.2. Polymer types of detected MPs

Samples from the remote sites (n = 9) contained mostly polyamide (49 %), polystyrene (18 %), and polyvinylester (13 %), while samples from the CUES site had mostly polyamide (30 %), PET (26 %), polyolefin (19 %), and polyvinylester (16 %) (Fig. 5). A two-way ANOVA test was conducted to test significant differences ($p < 0.05$) among the distribution of polymer types and MPs from fresh snow at remote sites, CUES, and remote summer snow samples. A significant difference ($p = 0.009$) was found between the polymer types among site types. There was also a significant difference ($p = 0.012$) in the distribution of the polymer types between site types. Therefore, the polymer types found at remote sites were significantly different than the polymer types found at the CUES site, where there were multiple local sources of MPs.

3.3. Morphology and size of detected MPs

Atmospheric MPs were observed and divided into two shapes, fragment and fiber. All 25 fibers observed were between 10–25 µm in thickness and 800–1600 µm in length. Of the 25 fibers, 15 were found at the CUES site. None were identified as plastic. This could be due to the size limitation of the µFTIR and the poor quality of spectra since it was near the limit of detection of the µFTIR (25 µm). Correlation matches with the Open Specy library with fibers were all below 0.7. Therefore, all MPs that had correlation factors of > 0.7 were of the fragment shape. The Feret diameter ratios for 99 % of the MP fragments were between 0.1 and 0.8. There was no significant difference ($p < 0.05$) between the four groups of samples and the distribution of the Feret diameters within

Table 2
Concentrations of MPs in snow.

Site Name	Date of Sampling	Event Snowfall (cm)	Snow Density (g/L)	Concentration of MPs in Meltwater (p/L)
Earthquake Dome 1	03/05/2022	6 cm	220	81.5
Earthquake Dome 2	03/05/2022	6 cm	220	151
Yost Meadow 1	03/06/2022	6 cm	200	20.9
Yost Meadow 2	03/06/2022	6 cm	200	24.7
Dana Plateau 1	02/28/2022	8 cm	210	5.08
Dana Plateau 2	02/28/2022	8 cm	210	60.5
TJ Lake	04/23/2022	28 cm	215	203
Tioga Pass	11/25/2021	N/A	N/A	138
Alaska	04/07/2022	N/A	N/A	20.5
CUES	4/12/2022	10 cm	215	149
CUES 1	4/26/2022	33 cm	215	242
CUES 2	4/26/2022	33 cm	215	317
CUES 3	4/26/2022	33 cm	215	325
CUES 1	01/7/2024	25 cm	158	105
CUES 2	01/7/2024	25 cm	158	154
CUES Pit	01/04/2022	100 −90 cm	334	267
CUES Pit	03/24/2022	60 −50 cm	417	146
CUES Pit	03/24/2022	110 −100 cm	399.5	913
CUES Pit	04/5/2022	55 −45 cm	490	35.1
Above Palmer Glacier	08/25/2021	N/A	N/A	121
Below Newton-Clark Glacier	08/27/2021	N/A	N/A	254
Conness Glacier	09/1/2023	N/A	N/A	539
Illumination Glacier 1	08/29/2021	N/A	N/A	91.2
Illumination Glacier 2	08/29/2021	N/A	N/A	57.5

those groups.

The majority (~90 %) of the MPs within each group were under 180 μm in Feret maximum diameter. There was no significant difference ($p < 0.05$) in size distribution among the sampling groups in this study. For the remote summer snow and CUES site samples, the greatest percentage of MPs (34–42 %) had a bin center of 50 μm. For remote fresh snow, the greatest percentage of particles (41 %) had a bin center of 100 μm.

4. Discussion

4.1. Distribution of microplastic concentrations in snow

In the small number MP occurrence in snowy environments investigations, the concentrations reported in snowy matrices are in a similar order of magnitude as wet and dry atmospheric deposition studies. [32–35] MP presence in remote mountainous snow contributes to understanding the fate and transport of atmospheric MPs. [51] The presence of MPs in remote areas confirms that there is a global long-range transport trend of MPs and therefore a global exposure to MPs. [43,45] It is difficult to compare the concentrations of particles/volume found in this study to studies that have lower size ranges (detection down to 5 μm using Raman spectroscopy), present concentrations in mass/volume values, and/or use different detection methods. Despite the lack of harmonization in relevant MP studies, comparisons may be made taking these factors into consideration. [52].

The concentrations of MPs found in this study ranged from 5.01–539 p/L of snow melt water (Table 2). There was a significant difference ($p = 0.038$) between MP concentrations in fresh snow sampled at remote sites and CUES, the site with local anthropogenic activity (Fig. 4). The MP concentrations observed in this study were almost two orders of magnitude lower than those reported in certain fresh snow studies from the Alps, Svalbard, and seasonal snow in Northeastern China. [2,18,53] Even CUES, the site with local anthropogenic sources in this study, had fresh snow concentrations of 104–539 p/L of meltwater, which were still much lower than the previously mentioned studies. Even though the CUES site does not have a local source of MPs like urban centers with 500,000 or more people, it is located at a ski resort where up to 20,000 people may be present and are covered in plastic materials during the winter and spring seasons. Site remoteness is comparable between the remote sites in this study and the sites in Svalbard and Northeastern China. The discrepancy in MP levels between this and the Alps, Svalbard, and seasonal snow in Northeastern China studies may be attributed to false positive MP identification since spectral libraries with limitations were used. For example, the spectral libraries may have extensive plastic spectra but no common false positive materials or aged plastic materials and thus may not have the wide

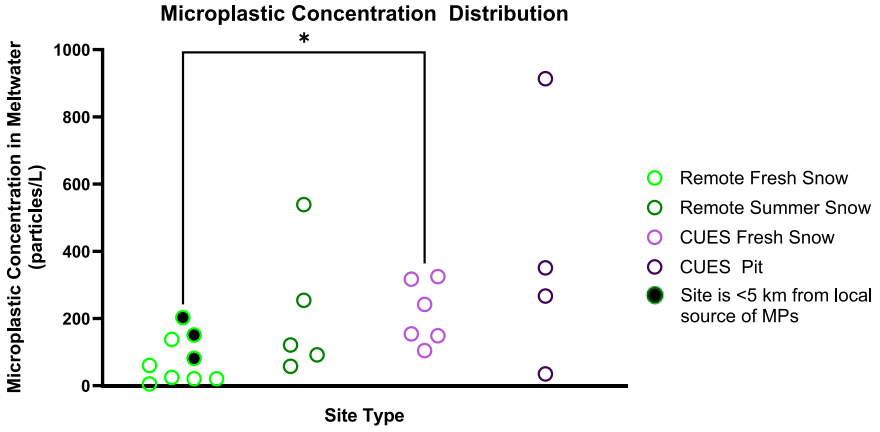

Fig. 4. Distribution of MP particles in snow (p/L). Sample sites were organized into four groups: remote fresh snow, remote summer snow, CUES fresh snow, and CUES pit. Solid black circles are sites that are < 5 km from a local anthropogenic source of MPs (population >5000).

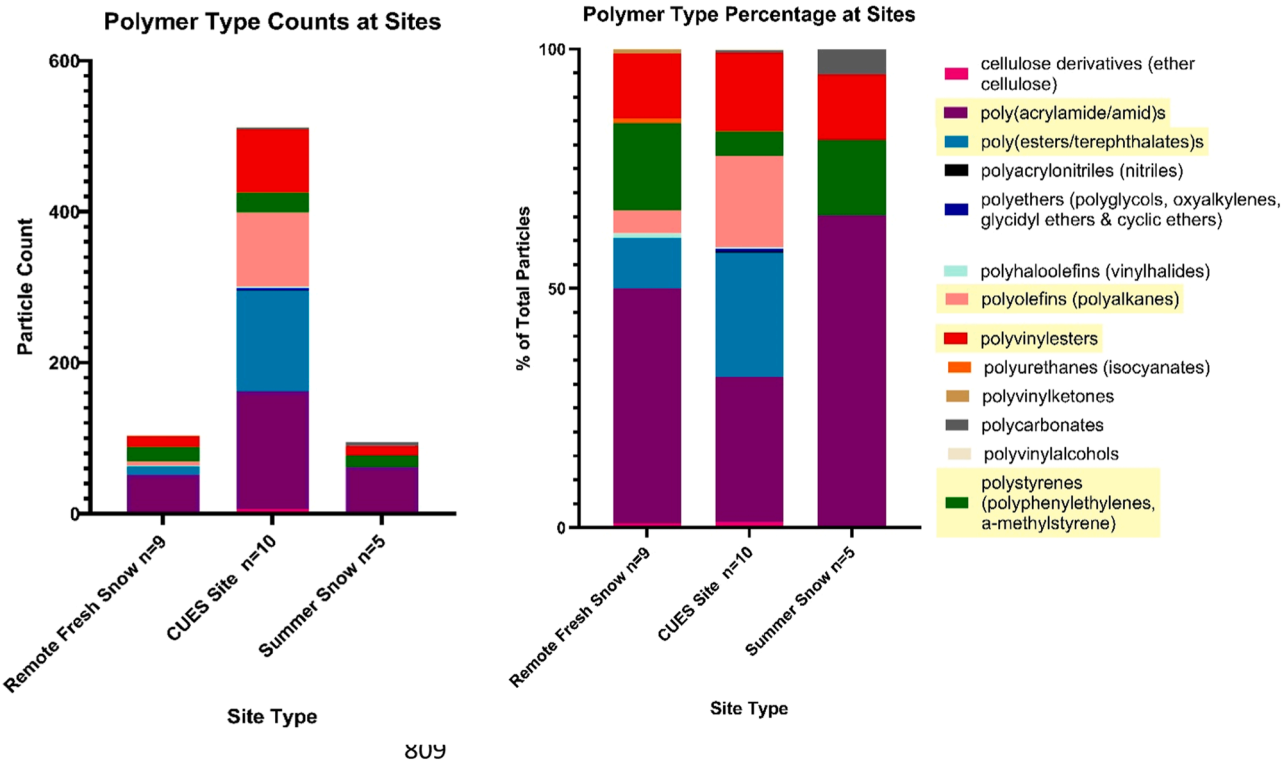

Fig. 5. Polymer type distribution among different sites. (A) Distribution of polymer types among sites as individual particle counts; (B) Distribution of polymer types among sites as fractions.

range of spectra as in Open Specy. Furthermore, the use of red Nile dye and fluorescent microscopy in some of these studies could cause the amount of MPs to be overestimated because of the tendency to dye organic material in addition to plastics. [54].

The concentrations of MPs found in the remote sites of this study were similar to the concentrations observed in fresh snow in the Inner Mongolian Plateau in China (68–199 p/L) and Carnic Alps in Italy (1–5 p/L) (Fig. 2). [37,38,55] The techniques used to detect MPs in those studies were Raman spectroscopy and μFTIR in a point-and-shoot method. The concentrations between those studies and the current study were comparable in that spectroscopy techniques were applied, and the detection limits were relatively similar. The sites on the Inner Mongolian Plateau were generally not very remote, and were near farmland, a hospital, a suburban area, a landfill, and a residential area. The concentrations reported from those sites were in the same order of magnitude as those observed in the current study where fresh snow was collected within 5 km of a significant source of MPs. The sites in the Carnic Alps were accessed with a system of ski-in and -out huts; in a similar fashion, many of the remote sites in the current study were accessed using backcountry ski touring equipment. Logically, the concentrations in this study closest to those reported in the Carnic Alps were those sampled from the remote backcountry sites. The study with the most similar method to the μFTIR mapping presented here, investigated snow in remote areas in Svalbard used Omnic Picta Particle Wizard (Thermofisher Scientific). In this study, the authors reported particle counts in the 50–100 μm size range in the same order of magnitude as that reported in our study (< 800 MPs/L). [56] Another study which also considered fresh snow in remote areas using μFTIR showed that remote sites in Japan had concentrations of 150–170 p/L. [57] The similarities in MP concentrations in fresh snow among remote sites suggest that sampling and detection techniques for MPs are improving and that there is a growing consensus in reported values of MP abundance in snow in remote sites at the global scale.

The concentrations found in this study were 1–2 orders of magnitude lower than what were reported from agricultural fields with plastic mulching or road dust with high counts of tire wear particles, where MP counts are in the thousands or tens of thousands per liter or kilogram. [58] The concentration range reported in this study is comparable to those found in rainfall and stormwater, where MP concentrations are reported to be under 1000 p/L. [59,60] The MP concentrations found in remote ice-covered parts of Lake Ulansuahi, a freshwater lake in inner Mongolia, were also comparable to the MP concentrations found in remote snow in this study (< 200 p/L). The MP concentrations detected in the ice above the lake were of the same order of magnitude as the concentrations found at the CUES site and summer snow, where long periods of dry deposition occur. [61] Environmental compartments with a similar magnitude of MP concentrations could be further explored using the workflow proposed in this study.

It is important to note that snow deposition accumulates as stratified layers within a seasonal snowpack. Bulk sampling of a snowpack will typically include both wet and dry deposition events that can be identified by differences in snow density in the snowpack. To understand the variability of MP concentrations within a snowpack, a set of samples were collected at different depths within the snowpack at CUES. From the snow pits dug at the CUES site, the MP concentrations varied from 35–913 p/L of meltwater (Fig. 4). The sample with the lowest MP presence had no dry deposition crusts present in the sample. The sample collected at 110–100 cm from the ground surface on 03/24/2022, had the highest concentration of MPs in meltwater at 913 p/L, included a crust layer of the longest dry period recorded in California history. [62] This indicates that gravitational deposition of MPs could potentially cause accumulation of MPs in the snowpack during extended dry periods. Under the context of climate change and a predicted increase in drought severity of California, gravitational deposition, in addition to cloud-scavenging of MPs, could be a significant contributor to MP occurrence in terrestrial environments. More pit sampling needs to be done to confirm that this is a seasonal pattern.

4.2. Morphology and size of microplastics in snow

At higher elevations, there is enhanced atmospheric deposition caused by lower temperature and higher precipitation rates during snowfall events. [63] For example, the CUES and California sites in this study are in the Sierra Nevada where snowfall accounts for 60–70 % of the annual precipitation. [64] The polymer types, MP size distribution, and frequency of the fragment shape in this study were similar to the results of studies on cloud water from the summits of mountains. [15,39] This may be due to the similarly high elevation of the cloud sampling sites (1252 m, 3776 m, and 1545 m) and similar methods of MP detection. Most particles detected in both the cloud water samples and in this study were under 100 μm in length and were dominated by fragment-shaped MPs. In other high-elevation MP studies like at Pic-du-Midi (2877 m) the ratio of fragment to fibers were 70 % and 30 %, respectively. [18] In this current study only 25 fibers were visually detected among all sites, and none were identified as plastic, as most had spectral matches with cellulose derivative classes with correlation values below 0.7. Of the 25 fibers, 19 were found in the CUES sites samples where there is a high amount of local anthropogenic activity. The reasoning for a lack of fiber dominance in the samples could be because under UV exposure fibers are known to degrade into fragments. [65] All the sites in the current study were at high elevations (> 2500 m) and therefore were under strong UV radiation creating a potential phenomenon where fibers released in the atmosphere matrix fragment quickly.

Presently, there seems to be stark differences in the most common shape type of MPs reported in atmospheric deposition studies. Some studies showed that samples were fiber dominant [33,66–69] in both urban and remote sites, and other studies found few to no fibers (<10 %). [15,39] Several factors may have contributed to the apparent differences. MP detection methods can have varying sensitivity for different particle shapes. Most textile fibers are under 25 μm in thickness may not be detected with methods that have detection limits above this size. In these cases, techniques with lower detection limits like pyrolysis-GC/MS or Raman spectroscopy may need to be used. Despite lack of MP fibers found in this study, it is estimated that the global emissions of MP fibers are estimated to be 6.5 ± 2.9 Tg annually and the deposition rate of MP fibers in North America are estimated to be 160 ± 71 kt. [23] With these estimations, we expect to see an increase of MP fiber presence in snow samples in subsequent studies.

Consistent with the literature, most of the MP particles found in this study were under 100 μm in size. Interestingly, the distribution of MP particle size was quite similar between the remote sites and sites with a localized MP source, as seen in the size distribution plots (Fig. 6). This was likely caused by the fact that as the size of MPs approached the detection limit on the FTIR, the spectral resolution diminished, and that it is unlikely for MP fragments > 100 μm to undergo atmospheric transport. It is expected that as the detection limit becomes lower, there will be an exponential increase in MP counts at the lower bin sizes (i.e. 10, 5, 1 μm). [70].

4.3. Polymer types of microplastics in snow

There also was a statistically significant difference ($p = 0.0089$) in the distribution of polymer types between the two site types (remote sites and CUES site). Remote sites were dominated by polyamides, polystyrenes, polyvinyl esters, and CUES, the site with localized sources of MPs, consisted mostly of polyamides, PET, polyolefins, and polyvinylesters (Fig. 5). Two-way ANOVA ($p < 0.05$) showed no significant differences among polymer types and their relative particle sizes. Although more samples over a longer period would be needed to further confirm this trend, the preliminary findings of this study suggested that small-sized MPs of polystyrene, polyamides, and polyvinylesters are more susceptible for long-range transport to remote areas.

According to Stokes' Law, long-range transport of MP particles is dependent on the density difference between the MP particle and the atmosphere, and the shape and size of the MP particle. Plastic materials can have a large range of densities, from 0.65–1.8 g cm^{-3}, and when plastic is manufactured as a foam material, particle densities can be reduced by up to an order of magnitude. [9] One reason that polystyrene may be a common polymer found in remote sites, is because polystyrene

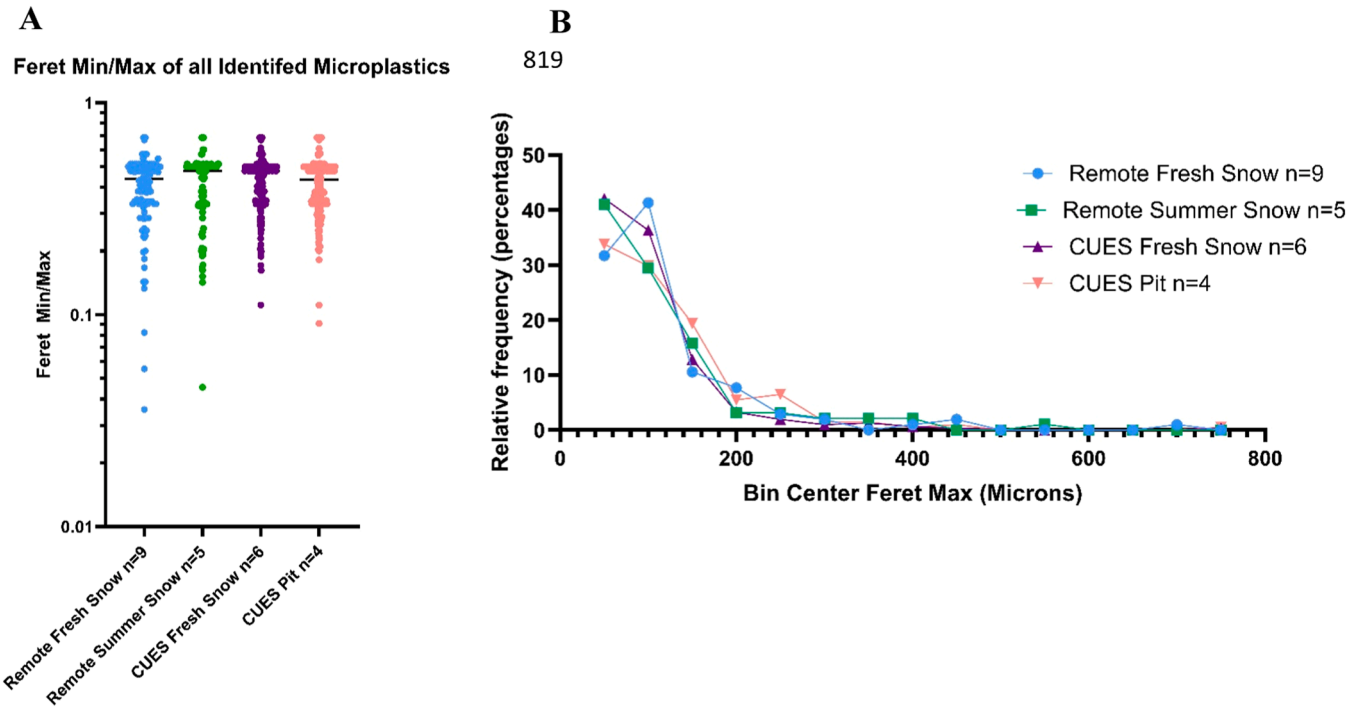

Fig. 6. Size distribution of MP particles among different site types. (A) Aspect ratio of identified MPs to determine particle shapes of identified MPs; (B) Distribution of Feret Max values among all identified particles.

foam is one of the lowest density plastic materials and therefore may have the greatest potential for long range transport. A recent study that sampled remote sites in Svalbard, also reported an abundance of polystyrene that was not present at the site with a localized source. [56] It is likely that polyamide MPs, specifically a spectral match with Nylon 66, were common at both remote sites and CUES, because polyamide was the most used plastic in these areas as it is found in outdoor and active gear. Another potential reason that polyamide is so common because polyamide is also the most common false positive for plant materials in μFTIR measurements. [28] One potential reason that polyamide is not commonly found as a fiber in this study is because fibers are known to fragment with aging, and so what could have started as a polyamide fiber could have been weathered and fragmented into smaller particles [71].

Global production of plastics by polymer types can be ranked as PP > LDPE > HDPE > PVC > PET > PS > PU. [72] This is not the same distribution as what is found in atmospheric samples. Thus far, there does not appear to be a consensus on what plastic polymer type is the most common in the atmosphere. This could be due to differences in sources of atmospheric MPs at the sampling sites, especially between urban and rural sites. The high variation in atmospheric MP polymer types reported to date could also be because of the lack of standardized methods, often the need to extrapolate data because of time-consuming methods, and variations in effective polymer spectral libraries. For example, on the Tibetan Plateau, rural sites had a distribution of polymers as PET (30.7 %), PE (17 %), PA (14.7 %), and PS (11 %), which differed from those observed in the current study. [73] Therefore, to discern patterns of atmospheric MPs, improved reporting and standardized methods for sample collection, preparation and detection are urgently needed. [74] Measurement of polymer additives and associated compounds such as UV-stabilizers, flame retardants, and even pesticides that could be co-transported with MPs may also provide insightful information to further evaluate the transport range of MPs through the atmosphere [75,76].

5. Conclusions

This study includes the first report of MP occurrence in fresh and seasonal summer snow across the West Coast of North America. Open Specy batch analysis allowed for a high-throughput method development that provides an opportunity to perform sample analyses on annual or seasonal timelines. Eleven sites covering approximately 4200 km in distance and 183–3292 m in elevation were visited. The concentrations of MPs found in the fresh snow of remote sites varied from 5.1–150.8 p/L of snowmelt water, while sites with a localized MP source (the CUES site) had concentrations of 104.5–539 p/L. The range of MP concentrations within the snowpack ranged from 35.1–913 p/L. The highest concentration of MPs was found at the end of the longest dry period recorded in the history of the CUES site location, at 913 p/L of meltwater. All particles identified as plastic were fragments, and most (~90 %) were under 200 μm. It was shown that there was a significant difference ($p = 0.0378$) in MP concentrations and polymer type distribution between CUES, the site with local anthropogenic activity, and remote mountain sites. The most common polymer types found at remote sites were polyamides, polystyrenes, and polyvinylesters. The most common polymer types of MPs found at the CUES site were polyamides, polyvinylesters, PET, and polyolefins.

There is a need for long-term monitoring of MPs, especially in the least studied yet critical environments like the atmosphere, where atmospheric processes drive the widespread transport of MP to remote environments. This study shows that MPs that are < 100 μm and are fragment-shaped have the potential to be atmospherically transported over long range distances. Seasonal and annual monitoring of atmospheric MPs can provide indication of the rate of transport and accumulation of MPs. Furthermore, Open Specy batch analysis allowed for the development of a high-throughput method suitable for sample analysis on annual or seasonal timelines. To further improve the detection limit of this workflow for smaller MPs (< 50 μm), a pyrolysis GC-MS may be used to determine presence and mass, or Raman spectroscopy with mapping capabilities could be added to this workflow. Additionally, it would be valuable to understand the reaches of anthropogenic pollution by concurrently characterizing man-made chemicals that are being co-transported with MPs, such as plastic and rubber additives.

Environmental implications

Microplastics can have hazardous implications to human and environmental health and have been found in every ecosystem. These particles can travel long ranges because of atmospheric transport and accumulation. This study detects microplastic presence in the snow in some of the first field observations across western coastal North America. The method used in this study - a combination of μFTIR mapping and Open Specy spectra batch analysis - is effectively used for high-throughput environmental sample analysis. The results of this study contribute to a better understanding of microplastic concentrations, polymer types, and sizes undergoing atmospheric deposition and demonstrate the need for long-term monitoring.

CRediT authorship contribution statement

Jay Gan: Writing – review & editing, Supervision, Funding acquisition, Conceptualization. **Andrew Gray:** Writing – review & editing, Supervision, Resources, Conceptualization. **Edward Bair:** Writing – original draft, Resources, Conceptualization. **Aleksandra Karapetrova:** Writing – original draft, Visualization, Formal analysis, Data curation, Conceptualization. **Audrey Braun:** Data curation. **Alex Michell:** Writing – review & editing, Data curation, Conceptualization. **Win Cowger:** Writing – review & editing, Resources, Methodology.

Declaration of Competing Interest

The authors declare that they have no known competing financial interests or personal relationships that could have appeared to influence the work reported in this paper.

Acknowledgements

Funding support was partially provided through the Pathfinder Fellowship granted by CUAHSI with support from the National Science Foundation (NSF) Cooperative Agreement (Grant No. EAR-1849458). The McPike Zima Charitable Foundation and the Cygnet Foundation funded the μFTIR time. E.B. received support from The National Aeronautics and Space Administration (Grant Nos. 80NSSC20K1722 and 80NSSC20K1349). A.G. was supported in part by the USDA National Institute of Food and Agriculture Hatch program (Project Number CA-R-ENS-5120-H), and USDA Multistate Project W4170 funds. The authors wish to thank Gwen Lattin and Matthew Dickson for technical assistance.

Data availability

A data repository can be found at DOI 10.5281/zenodo.13877243.

References

[1] Aves, A.R., Revell, L.E., Gaw, S., Ruffell, H., Schuddeboom, A., Wotherspoon, N.E., LaRue, M., McDonald, A.J., 2022. First evidence of microplastics in antarctic snow. Cryosphere 16 (6), 2127–2145. https://doi.org/10.5194/tc-16-2127-2022.

[2] Bergmann, M., Mützel, S., Primpke, S., Tekman, M.B., Trachsel, J., Gerdts, G., 2019. White and Wonderful? Microplastics prevail in snow from the Alps to the Arctic. Sci Adv 5 (8), eaax1157. https://doi.org/10.1126/sciadv.aax1157.

[3] Allen, S., Allen, D., Phoenix, V.R., Le Roux, G., Durántez Jiménez, P., Simonneau, A., Binet, S., Galop, D., 2019. Atmospheric transport and deposition of microplastics in a remote mountain catchment. Nat Geosci 12 (5), 339–344. https://doi.org/10.1038/s41561-019-0335-5.

[4] Ritchie, H., Roser, M., 2018. Our world data. Plast Pollut.

[5] Geyer, R., Jambeck, J.R., Law, K.L., 2017. Production, use, and fate of all plastics ever made. Sci Adv 3 (7), e1700782. https://doi.org/10.1126/sciadv.1700782.

[6] OECD. Global Plastics Outlook: Policy Scenarios to 2060; Organisation for Economic Co-operation and Development: Paris, 2022.

[7] Luo, X., Wang, Z., Yang, L., Gao, T., Zhang, Y., 2022. A review of analytical methods and models used in atmospheric microplastic research. Sci Total Environ 828, 154487. https://doi.org/10.1016/j.scitotenv.2022.154487.

[8] Rochman, C.M., 2018. Microplastics research—from sink to source. Science 360 (6384), 28–29. https://doi.org/10.1126/science.aar7734.

[9] Abad López, A.P.; Trilleras, J.; Arana, V.A.; Garcia-Alzate, L.S.; Grande-Tovar, C.D. Atmospheric Microplastics: Exposure, Toxicity, and Detrimental Health Effects. RSC Adv. 13 (11), 7468–7489. https://doi.org/10.1039/d2ra07098g.

[10] Gasperi, J., Wright, S.L., Dris, R., Collard, F., Mandin, C., Guerrouache, M., Langlois, V., Kelly, F.J., Tassin, B., 2018. Microplastics in air: are we breathing it in? Curr Opin Environ Sci Health 1, 1–5. https://doi.org/10.1016/j.coesh.2017.10.002.

[11] Xu, A., Shi, M., Xing, X., Su, Y., Li, X., Liu, W., Mao, Y., Hu, T., Qi, S., 2022. Status and prospects of atmospheric microplastics: a review of methods, occurrence, composition, source and health risks. Environ Pollut 303, 119173. https://doi.org/10.1016/j.envpol.2022.119173.

[12] Beyer, A., Mackay, D., Matthies, M., Wania, F., Webster, E., 2000. Assessing long-range transport potential of persistent organic pollutants. Environ Sci Technol 34 (4), 699–703. https://doi.org/10.1021/es990207w.

[13] McLachlan, M.S., Sellström, U., 2009. Precipitation scavenging of particle-bound contaminants – a case study of PCDD/Fs. Atmos Environ 43 (38), 6084–6090. https://doi.org/10.1016/j.atmosenv.2009.08.037.

[14] Aeschlimann, M., Li, G., Kanji, Z.A., Mitrano, D.M., 2022. Potential impacts of atmospheric microplastics and nanoplastics on cloud formation processes. Nat Geosci 15 (12), 967–975. https://doi.org/10.1038/s41561-022-01051-9.

[15] Wang, Y., Okochi, H., Tani, Y., Hayami, H., Minami, Y., Katsumi, N., Takeuchi, M., Sorimachi, A., Fujii, Y., Kajino, M., Adachi, K., Ishihara, Y., Iwamoto, Y., Niida, Y., 2023. Airborne hydrophilic microplastics in cloud water at high altitudes and their role in cloud formation. Environ Chem Lett 21 (6), 3055–3062. https://doi.org/10.1007/s10311-023-01626-x.

[16] Bain, A., Preston, T.C., 2021. Hygroscopicity of microplastic and mixed microplastic aqueous ammonium sulfate systems. Environ Sci Technol 55 (17), 11775–11783. https://doi.org/10.1021/acs.est.1c04272.

[17] Lei, Y.D., Wania, F., 2004. Is rain or snow a more efficient scavenger of organic chemicals? Atmos Environ 38 (22), 3557–3571. https://doi.org/10.1016/j.atmosenv.2004.03.039.

[18] Allen, S., Allen, D., Baladima, F., Phoenix, V.R., Thomas, J.L., Le Roux, G., Sonke, J.E., 2021. Evidence of free tropospheric and long-range transport of microplastic at pic Du midi observatory. Nat Commun 12 (1), 7242. https://doi.org/10.1038/s41467-021-27454-7.

[19] Zhao, S., Yu, Y., He, J., Yin, D., Wang, B., 2015. Below-cloud scavenging of aerosol particles by precipitation in a typical valley City, Northwestern China. Atmos Environ 102, 70–78. https://doi.org/10.1016/j.atmosenv.2014.11.051.

[20] Gouin, T., 2021. Addressing the importance of microplastic particles as vectors for long-range transport of chemical contaminants: perspective in relation to prioritizing research and regulatory actions. Micro Nanoplastics 1 (1), 14. https://doi.org/10.1186/s43591-021-00016-w.

[21] Brahney, J., Mahowald, N., Prank, M., Cornwell, G., Klimont, Z., Matsui, H., Prather, K.A., 2021. Constraining the atmospheric limb of the plastic cycle. Proc Natl Acad Sci 118 (16). https://doi.org/10.1073/pnas.2020719118.

[22] Evangeliou, N., Grythe, H., Klimont, Z., Heyes, C., Eckhardt, S., Lopez-Aparicio, S., Stohl, A., 2020. Atmospheric transport is a major pathway of microplastics to remote regions. Nat Commun 11 (1), 3381. https://doi.org/10.1038/s41467-020-17201-9.

[23] Evangeliou, N., Tichý, O., Eckhardt, S., Zwaaftink, C.G., Brahney, J., 2022. Sources and fate of atmospheric microplastics revealed from inverse and dispersion modelling: from global emissions to deposition. J Hazard Mater 432, 128585. https://doi.org/10.1016/j.jhazmat.2022.128585.

[24] King, K.E., Cook, E.R., Anchukaitis, K.J., Cook, B.I., Smerdon, J.E., Seager, R., Harley, G.L., Spei, B., 2024. Increasing prevalence of hot drought across Western North America since the 16th century. Sci Adv 10 (4), eadj4289. https://doi.org/10.1126/sciadv.adj4289.

[25] *A "Surprisingly Average" Year for Sierra Snowpack*. ⟨https://earthobservatory.nasa.gov/images/152673/a-surprisingly-average-year-for-sierra-snowpack⟩ (accessed 2024–05-05).

[26] Schmidt, C., Krauth, T., Wagner, S., 2017. Export of plastic debris by rivers into the sea. Environ Sci Technol 51 (21), 12246–12253. https://doi.org/10.1021/acs.est.7b02368.

[27] Bank, M.S., Hansson, S.V., 2022. The Microplastic Cycle: An Introduction to a Complex Issue. In: Bank, M.S. (Ed.), Microplastic in the Environment: Pattern and Process. Springer International Publishing, Cham, pp. 1–16. https://doi.org/10.1007/978-3-030-78627-4_1.

[28] Roscher, L., Halbach, M., Nguyen, M.T., Hebeler, M., Luschtinetz, F., Scholz-Böttcher, B.M., Primpke, S., Gerdts, G., 2022. Microplastics in two German wastewater treatment plants: year-long effluent analysis with FTIR and Py-GC/MS. Sci Total Environ 817, 152619. https://doi.org/10.1016/j.scitotenv.2021.152619.

[29] Liu, Y., Jiang, W.-Y., Liao, Y., Sun, R., Hu, J., Lu, Z., Chang, M., Yang, J., Dai, Z., Zhou, C., Hong, P., Qian, Z.-J., Sun, S., Ren, L., Liang, Y.-Q., Zhang, Y., Li, C., 2022. Separation of false-positive microplastics and analysis of microplastics via a two-phase system combined with confocal raman spectroscopy. J Hazard Mater 440, 129803. https://doi.org/10.1016/j.jhazmat.2022.129803.

[30] Song, Z., Zhang, L., Tian, C., Li, K., Chen, P., Jia, Z., Hu, P., Cui, S., 2024. Chemical characteristics, distribution patterns, and source apportionment of particulate elements and inorganic ions in snowpack in Harbin, China. Chemosphere 349, 140886. https://doi.org/10.1016/j.chemosphere.2023.140886.

[31] Thornton Hampton, L.M., De Frond, H., Gesulga, K., Kotar, S., Lao, W., Matuch, C., Weisberg, S.B., Wong, C.S., Brander, S., Christansen, S., Cook, C.R., Du, F., Ghosal, S., Gray, A.B., Hankett, J., Helm, P.A., Ho, K.T., Kefela, T., Lattin, G., Lusher, A., Mai, L., McNeish, R.E., Mina, O., Minor, E.C., Primpke, S., Rickabaugh, K., Renick, V.C., Singh, S., van Bavel, B., Vollnhals, F., Rochman, C. M., 2023. The influence of complex matrices on method performance in extracting and monitoring for microplastics. Chemosphere 334, 138875. https://doi.org/10.1016/j.chemosphere.2023.138875.

[32] González-Pleiter, M., Edo, C., Aguilera, Á., Viúdez-Moreiras, D., Pulido-Reyes, G., González-Toril, E., Osuna, S., de Diego-Castilla, G., Leganés, F., Fernández-Piñas, F., Rosal, R., 2021. Occurrence and transport of microplastics sampled within and above the planetary boundary layer. Sci Total Environ 761, 143213. https://doi.org/10.1016/j.scitotenv.2020.143213.

[33] Zhang, Y., Kang, S., Allen, S., Allen, D., Gao, T., Sillanpää, M., 2020. Atmospheric microplastics: a review on current status and perspectives. Earth-Sci Rev 203, 103118. https://doi.org/10.1016/j.earscirev.2020.103118.

[34] Le, V.-G., Nguyen, M.-K., Nguyen, H.-L., Lin, C., Hadi, M., Hung, N.T.Q., Hoang, H.-G., Nguyen, K.N., Tran, H.-T., Hou, D., Zhang, T., Bolan, N.S., 2023. A Comprehensive review of micro- and nano-plastics in the atmosphere: occurrence, fate, toxicity, and strategies for risk reduction. Sci Total Environ 904, 166649. https://doi.org/10.1016/j.scitotenv.2023.166649.

[35] Can-Güven, E., 2020. Microplastics as emerging atmospheric pollutants: a review and bibliometric analysis. Air Qual Atmosphere Health. https://doi.org/10.1007/s11869-020-00926-3.

[36] Napper, I.E., Davies, B.F.R., Clifford, H., Elvin, S., Koldewey, H.J., Mayewski, P.A., Miner, K.R., Potocki, M., Elmore, A.C., Gajurel, A.P., Thompson, R.C., 2020. Reaching new heights in plastic pollution—preliminary findings of microplastics on mount everest. One Earth 3 (5), 621–630. https://doi.org/10.1016/j.oneear.2020.10.020.

[37] Pastorino, P., Pizzul, E., Bertoli, M., Anselmi, S., Kušće, M., Menconi, V., Prearo, M., Renzi, M., 2021. First insights into plastic and microplastic occurrence in biotic and abiotic compartments, and snow from a high-mountain lake (Carnic Alps). Chemosphere 265, 129121. https://doi.org/10.1016/j.chemosphere.2020.129121.

[38] Zhang, Y., Kang, S., Luo, X., Shukla, T., Gao, T., Allen, D., Allen, S., Bergmann, M., 2023. Microplastics and nanoplastics pose risks on the Tibetan plateau environment. Sci Bull. https://doi.org/10.1016/j.scib.2023.12.015.

[39] Xu, X., Li, T., Zhen, J., Jiang, Y., Nie, X., Wang, Y., Yuan, X.-Z., Wang, X., Xue, L., Chen, J., 2023. Characterization of microplastics in clouds over eastern China. Environ Sci Technol Lett. https://doi.org/10.1021/acs.estlett.3c00729.

[40] Primpke, S., Lorenz, C., Rascher-Friesenhausen, R., Gerdts, G., 2017. An automated approach for microplastics analysis using focal plane array (FPA) FTIR microscopy and image analysis. Anal Methods 9 (9), 1499–1511. https://doi.org/10.1039/C6AY02476A.

[41] da Silva, V.H., Murphy, F., Amigo, J.M., Stedmon, C., Strand, J., 2020. Classification and quantification of microplastics (<100 Mm) using a focal plane array–fourier transform infrared imaging system and machine learning. Anal Chem 92 (20), 13724–13733. https://doi.org/10.1021/acs.analchem.0c01324.

[42] Primpke, S., Godejohann, M., Gerdts, G., 2020. Rapid identification and quantification of microplastics in the environment by quantum cascade laser-based hyperspectral infrared chemical imaging. Environ Sci Technol 54 (24), 15893–15903. https://doi.org/10.1021/acs.est.0c05722.

[43] Evangeliou, N., Grythe, H., Klimont, Z., Heyes, C., Eckhardt, S., Lopez-Aparicio, S., Stohl, A., 2020. Atmospheric transport is a major pathway of microplastics to remote regions. Nat Commun 11 (1), 3381. https://doi.org/10.1038/s41467-020-17201-9.

[44] Cowger, W., Steinmetz, Z., Gray, A., Munno, K., Lynch, J., Hapich, H., Primpke, S., De Frond, H., Rochman, C., Herodotou, O., 2021. Microplastic spectral classification needs an open source community: open specy to the rescue! Anal Chem 93 (21), 7543–7548. https://doi.org/10.1021/acs.analchem.1c00123.

[45] Allen, S., Allen, D., Phoenix, V.R., Le Roux, G., Durántez Jiménez, P., Simonneau, A., Binet, S., Galop, D., 2019. Atmospheric transport and deposition of microplastics in a remote mountain catchment. Nat Geosci 12 (5), 339–344. https://doi.org/10.1038/s41561-019-0335-5.

[46] Bair, E.H., Davis, R.E., Dozier, J., 2018. Hourly mass and snow energy balance measurements from Mammoth Mountain, CA USA, 2011–2017. Earth Syst Sci Data 10 (1), 549–563. https://doi.org/10.5194/essd-10-549-2018.

[47] *Annual 2022 Drought Report | National Centers for Environmental Information (NCEI)*. ⟨https://www.ncei.noaa.gov/access/monitoring/monthly-report/drought/202213⟩ (accessed 2024–07-08).

[48] Cowger, W., Steinmetz, Z., Leong, N., Faltynkova, A., Sherrod, H., 2024. OpenSpecy: analyze, process, identify, and share Raman and (FT)IR spectra. R Package Version 1 1 0. ⟨https://CRAN.R-project.org/package=OpenSpecy⟩.

[49] Karapetrova, A. Exploring Microplastic Distribution in Western American Snow, 2024. https://doi.org/10.5281/zenodo.13877244.

[50] Cai, H., Du, F., Li, L., Li, B., Li, J., Shi, H., 2019. A practical approach based on FT-IR spectroscopy for identification of semi-synthetic and natural celluloses in

microplastic investigation. Sci Total Environ 669, 692–701. https://doi.org/10.1016/j.scitotenv.2019.03.124.
[51] Wei, Y., Yu, Y., Cao, X., Wang, B., Yu, D., Wang, J., Liu, Z., 2024. Remote mountainous area inevitably becomes temporal sink for microplastics driven by atmospheric transport. Environ Sci Technol. https://doi.org/10.1021/acs.est.4c00296.
[52] Lusher, A.L., Munno, K., Hermabessiere, L., Carr, S., 2020. Isolation and extraction of microplastics from environmental samples: an evaluation of practical approaches and recommendations for further harmonization. Appl Spectrosc 74 (9), 1049–1065. https://doi.org/10.1177/0003702820938993.
[53] Wen, H., Xu, H., Ma, Y., Zhang, C., Zhang, D., Wang, X., 2024. Diverse and high pollution of microplastics in seasonal snow across northeastern China. Sci Total Environ 907, 167923. https://doi.org/10.1016/j.scitotenv.2023.167923.
[54] Stanton, T., Johnson, M., Nathanail, P., Gomes, R.L., Needham, T., Burson, A., 2019. Exploring the efficacy of nile red in microplastic quantification: a costaining approach. Environ Sci Technol Lett 6 (10), 606–611. https://doi.org/10.1021/acs.estlett.9b00499.
[55] Yu, H., Shao, J., Jia, H., Gang, D., Ma, B., Hu, C., 2023. Characteristics and influencing factors of microplastics in snow in the inner Mongolia Plateau, China. Engineering. https://doi.org/10.1016/j.eng.2023.02.007.
[56] Rosso, B., Scoto, F., Hallanger, I.G., Larose, C., Gallet, J.C., Spolaor, A., Bravo, B., Barbante, C., Gambaro, A., Corami, F., 2024. Characteristics and quantification of small microplastics (<100 Mm) in seasonal svalbard snow on glaciers and lands. J Hazard Mater 467, 133723. https://doi.org/10.1016/j.jhazmat.2024.133723.
[57] Ohno, H., Iizuka, Y., 2023. Microplastics in snow from protected areas in Hokkaido, the Northern Island of Japan. Sci Rep 13 (1), 9942. https://doi.org/10.1038/s41598-023-37049-5.
[58] Campanale, C., Galafassi, S., Savino, I., Massarelli, C., Ancona, V., Volta, P., Uricchio, V.F., 2022. Microplastics pollution in the terrestrial environments: poorly known diffuse sources and implications for plants. Sci Total Environ 805, 150431. https://doi.org/10.1016/j.scitotenv.2021.150431.
[59] Villafañe, A.B., Ronda, A.C., Rodríguez Pirani, L.S., Picone, A.L., Lucchi, L.D., Romano, R.M., Pereyra, M.T., Arias, A.H., 2023. Microplastics and Anthropogenic Debris in Rainwater from Bahia Blanca, Argentina. Heliyon 9 (6), e17028. https://doi.org/10.1016/j.heliyon.2023.e17028.
[60] Abbasi, S., 2021. Microplastics washout from the atmosphere during a monsoon rain event. J Hazard Mater Adv 4, 100035. https://doi.org/10.1016/j.hazadv.2021.100035.
[61] Liu, Y., Shi, X., Zhang, S., Lu, J., Li, W., Sun, B., Zhao, S., Yao, D., Huotari, J., 2023. The spatial distribution and abundance of microplastics in Lake waters and ice during ice-free and ice-covered periods. Environ Pollut 323, 121268. https://doi.org/10.1016/j.envpol.2023.121268.
[62] 2022 *Is California's Driest Year on Record So Far – an Ominous Sign for Summer and Fall | Weather.com*. ⟨https://weather.com/news/climate/news/2022–05-09-california-record-dry-year-to-date⟩ (accessed 2024–07-24).
[63] Daly, G.L., Wania, F., 2005. Organic contaminants in mountains. Environ Sci Technol 39 (2), 385–398. https://doi.org/10.1021/es048859u.
[64] *A Long View of Sierra Snow*. ⟨https://earthobservatory.nasa.gov/images/148595/a-long-view-of-sierra-snow⟩ (accessed 2024–07-24).
[65] Sørensen, L., Groven, A.S., Hovsbakken, I.A., Del Puerto, O., Krause, D.F., Sarno, A., Booth, A.M., 2021. UV degradation of natural and synthetic microfibers causes fragmentation and release of polymer degradation products and chemical additives. Sci Total Environ 755, 143170. https://doi.org/10.1016/j.scitotenv.2020.143170.
[66] Abbasi, S., Turner, A., 2021. Dry and wet deposition of microplastics in a semi-arid region (Shiraz, Iran). Sci Total Environ 786, 147358. https://doi.org/10.1016/j.scitotenv.2021.147358.
[67] Brahney, J., Hallerud, M., Heim, E., Hahnenberger, M., Sukumaran, S., 2020. Plastic rain in protected areas of the United States. Science 368 (6496), 1257–1260. https://doi.org/10.1126/science.aaz5819.
[68] Wright, S.L., Ulke, J., Font, A., Chan, K.L.A., Kelly, F.J., 2020. Atmospheric microplastic deposition in an urban environment and an evaluation of transport. Environ Int 136, 105411. https://doi.org/10.1016/j.envint.2019.105411.
[69] Wang, X., Li, C., Liu, K., Zhu, L., Song, Z., Li, D., 2020. Atmospheric microplastic over the south china sea and east Indian Ocean: abundance, distribution and source. J Hazard Mater 389, 121846. https://doi.org/10.1016/j.jhazmat.2019.121846.
[70] Kooi, M., Koelmans, A.A., 2019. Simplifying microplastic via continuous probability distributions for size, shape, and density. Environ Sci Technol Lett 6 (9), 551–557. https://doi.org/10.1021/acs.estlett.9b00379.
[71] Pinlova, B., Nowack, B., 2023. Characterization of fiber fragments released from polyester textiles during UV weathering. Environ Pollut, 121012. https://doi.org/10.1016/j.envpol.2023.121012.
[72] *Global primary plastic production by polymer*. Our World in Data. ⟨https://ourworldindata.org/grapher/plastic-production-polymer⟩ (accessed 2024–05-09).
[73] Luo, D., Wang, Z., Liao, Z., Chen, G., Ji, X., Sang, Y., Qu, L., Chen, Z., Wang, Z., Dahlgren, R.A., Zhang, M., Shang, X., 2024. Airborne microplastics in urban, rural and wildland environments on the Tibetan Plateau. J Hazard Mater 465, 133177. https://doi.org/10.1016/j.jhazmat.2023.133177.
[74] Beaurepaire, M., Dris, R., Gasperi, J., Tassin, B., 2021. Microplastics in the atmospheric compartment: a comprehensive review on methods, results on their occurrence and determining factors. Curr Opin Food Sci 41, 159–168. https://doi.org/10.1016/j.cofs.2021.04.010.
[75] Silva, A.O.D., Young, J., Spencer, C., Muir, C.; G., D, C., Sharp, M., Lehnherr, I., Criscitiello, A., 2023. Canadian high arctic ice core records of organophosphate flame retardants and plasticizers. Environ Sci Process Impacts 25 (12), 2001–2014. https://doi.org/10.1039/D3EM00215B.
[76] MacInnis, J.J., French, K., Muir, D.C.G., Spencer, C., Criscitiello, A., De Silva, A.O., Young, C.J., 2017. Emerging investigator series: a 14-year depositional ice record of perfluoroalkyl substances in the high Arctic. Environ Sci Process Impacts 19 (1), 22–30. https://doi.org/10.1039/C6EM00593D.